Computational Millimeter Wave Imaging: Problems, Progress and Prospects

Vishal M. Patel, Joseph N. Mait, Dennis W. Prather, and Abigail S. Hedden

Abstract

Imaging using millimeter waves (mmWs) has many advantages and applications in the defense, security and aviation markets. All terrestrial bodies emit mmW radiation and these wavelengths are able to penetrate smoke, blowing dust or sand, fog/clouds/marine layers, and even clothing. However there are many obstacles to imaging in this spectrum that one has to overcome before mmW imaging systems can be successfully realized for surveillance and defense applications. Recent developments in computational imaging have the potential to significantly improve capabilities of mmW imaging systems. Our paper will provide an overview of computational imaging and their implication to mmW imaging in various operation modes. We will discuss the merits and drawbacks of available computational mmW imaging approaches and identify avenues of research in this rapidly evolving field.

Index Terms

Millimeter wave imaging, computational imaging, surveillance, image reconstruction, image enhancement, extended depth of field.

I. Introduction

In the past several years, interest in imaging at millimeter wavelengths has been driven primarily by their ability to penetrate poor weather and other obscurants, such as clothes and polymers [1], [2]. Within the electromagnetic spectrum, millimeter waves are historically defined in the 30 to 300 GHz

Vishal M. Patel is with the department of Electrical and Computer Engineering at Rutgers University, Piscataway, NJ USA vishal.m.patel@rutgers.edu.

Joseph N. Mait and Abigail S. Hedden are with the U.S. Army Research Laboratory, Adelphi, MD USA {joseph.n.mait2.civ, abigail.s.hedden.civ}@mail.mil

Dennis W. Prather is with the Department of Electrical and Computer Engineering at the University of Delaware, Newark, DE USA dprather@udel.edu.

range with corresponding wavelengths between 10 to 1 mm, respectively. Radiation at these frequencies is non-ionizing and is therefore considered safe for human exposure. Applications of this technology include the detection of concealed weapons, explosives, and contraband (see Figure 1). Furthermore, unlike visible and infrared systems, passive mmW imaging systems are not significantly hindered by atmospheric obscurants, such as cloud cover, fog, smoke, rain and dust storms and may reduce, or even eliminate, the impact of low-visibility atmospheric conditions [3]. Figure 2 shows atmospheric attenuation of naturally emitted black-body radiation through 1 km of fog illustrating how low loss bands within the mmW region allow passive imaging in adverse weather conditions.

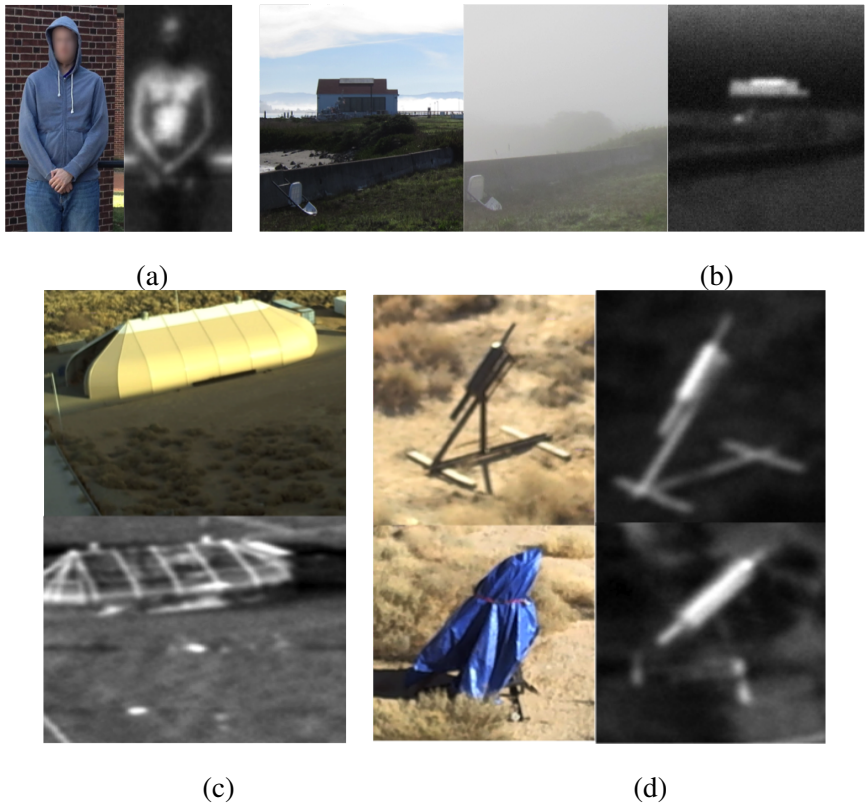

Fig. 1: Applications of mmW imaging. (a) Imaging through clothing. (b) Imaging through fog. (c) Imaging through tarps and building materials. (d) Imaging IRAM through canvas.

Unfortunately, mmW imaging combines the worst of radio frequency imaging and visible imaging. Consider that measuring phase at radio frequencies and measuring intensity at visible wavelengths are simple and inexpensive. However, measuring phase and measuring intensity are both expensive at mmWs. This is due primarily to the small signal-to-noise ratios that exist for passive mmW sources. Further, no

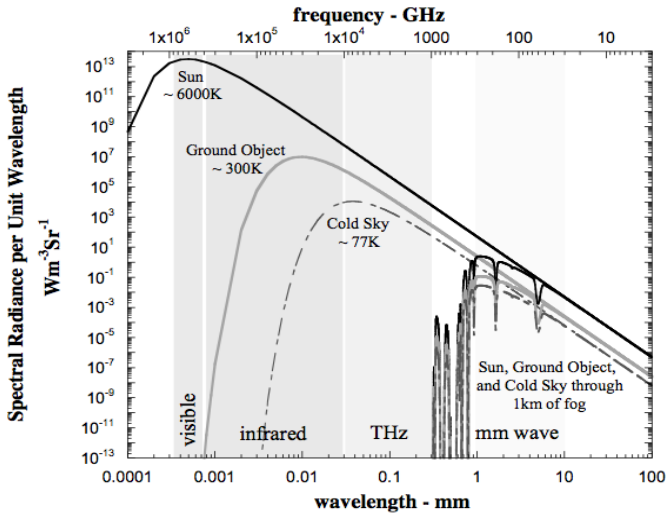

Fig. 2: Low loss bands within the mmW region allow passive imaging in adverse weather conditions [4].

large-scale integrated detector arrays exist for millimeter waves. In fact, at 100 GHz, there are only order 200×200 resolution elements across an 60×60-cm^2 aperture. Man-portable mega-pixel imagers at millimeter waves will be difficult to realize.

In light of the fact that the magnitude of mmW measurements is considerably less than that of visible measurements and that each measurement is expensive, one would like to increase the information content in the measurements that one does make. This requires methods beyond conventional imaging and leads us naturally to consider computational imaging techniques. In computational imaging, the burden of image formation is shared across two domains, the optical measurement and the digital post-processing domains. The opportunities for computational imaging depend upon the architecture of the system [4]–[13]. In this article, we review work that we have done for conventional imagers and for pupil, or Fourier plane, imagers.

This paper is organized as follows. In Section II we review the fundamentals of computational imaging. Recent computational mmW imaging methods are surveyed in Section III. Finally, concluding remarks are made in Section IV .

II. Foundations of Computational Imaging

Figure 3 is a schematic representation of a generic imaging system. To the left of the entrance pupil exists a natural scene consisting of self-luminous objects or objects illuminated passively, i.e., we do

not have active control over the scene illumination. The electromagnetic field incident upon the entrance pupil exists in three spatial dimensions (x, y, z) and one temporal dimension t and exhibits intrinsic physical properties of wavelength λ and polarization p. The amplitude of the field is represented by $a(x, y, z, t, \lambda, p)$.

All elements to the right of the entrance pupil are under a designer's control and together define the imaging system. The imager's front end contains elements that manipulate the incident wavefront. The front end electromagnetic processing is represented by linear, continuous integral transforms based on physical models.

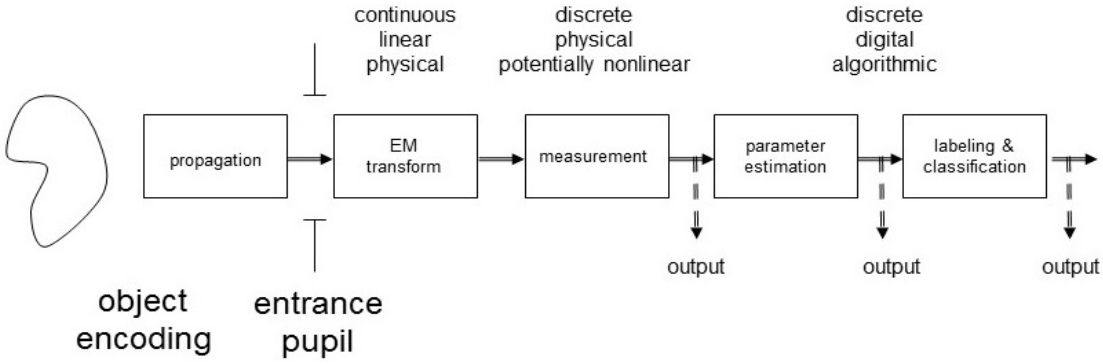

Fig. 3: Schematic representation of an imaging system.

After manipulation by the front end, the transformed wavefront impinges on a detector or transducer of some kind. Transduction is a nonlinear physical process in terms of field amplitude. It is the irradiance of the field that is transduced, $f = |a|^2$. Also, discrete sampling is implicit in transduction. The continuous values (x, y, z, t, λ, p) over which f is defined are now discrete.

One can use a matrix representation to provide a mathematical description of the processes up to and including measurement [14], [15]

$$\mathbf{g} = \mathbf{H}\mathbf{f} + \mathbf{n}, \tag{1}$$

where $\mathbf{g}$ is the measurement, $\mathbf{f}$ is a sampled representation of the scene irradiance in the object domain, $\mathbf{H}$ is the system transfer or measurement matrix, and $\mathbf{n}$ is noise introduced in the measurement process. The propagation of $\mathbf{f}$ from the object domain to the imager is included in $\mathbf{H}$. Thus, $\mathbf{H}$ consists of both natural and engineered components.

One applies a parameter estimator $\mathbf{T}$ in post-detection either to estimate $\mathbf{f}$ or some property, or

parameter, of $\mathbf{f}$ denoted $\mathbf{\Omega f}$, i.e., either

$$\begin{aligned} \hat{\mathbf{f}} &= \mathbf{Tg}, \\ &= \mathbf{THf} + \mathbf{Tn}, \end{aligned} \tag{2}$$

or

$$\begin{aligned} \Omega\mathbf{f} &= \mathbf{Tg}, \\ &= \mathbf{THf} + \mathbf{Tn}. \end{aligned} \tag{3}$$

In contrast to the measurement matrix $\mathbf{H}$, which operates linearly on $\mathbf{f}$, $\mathbf{T}$ can be linear or nonlinear.

The last block in Figure 3 represents additional processing beyond estimation, namely, labeling or classification. That is, based upon the properties estimated, elements within the scene are discriminated from one another and assigned to a particular, discrete class of objects. Depending upon the application, classification may not be necessary. We combine classification processing with estimation into a single transformation $\mathbf{T}$.

It is important to note the special case of $\mathbf{T} = \mathbf{I}$, where $\mathbf{I}$ is the identity matrix. This is called a direct measurement, where the measurements correspond directly the parameters of interest. For example, conventional imaging is a case of direct measurement of scene irradiance values in object space. The goal in designing a conventional imaging system is to produce a response that is as close as possible to a δ-function over all expected operating conditions.

Another classic example of direct measurement is optical matched filtering, e.g. [16]. One designs a matched filter to detect an object $\mathbf{o}$ in the object scene. Its ideal performance is such that, where ever $\mathbf{o}$ is present in the scene $\mathbf{f}$, the measurement produces a large response at its location. Locations where $\mathbf{o}$ is not present produce a small response. Thus, $\mathbf{T}$ outputs the location of $\mathbf{o}$ and, by virtue of its design, allows one to classify points in the scene $\mathbf{f}$ into two regions, those that likely contain $\mathbf{o}$ and those that don't.

These examples represent extremes in which all processing is performed in the physical domain. The vast expanse of work in optical design speaks to the difficulty in realizing the former and the short-lived history of optical pattern recognition in the 1960s and 1970s underscores problems with the latter. Thus, the application space of current interest is the one in which the processing burden is shared.

We delineate computational imaging into three broad applications: enhancing cameras, enhancing images (also known as computational photography), and enhancing human cognition. Reference to cameras in the first application emphasizes the conventional notion of a camera as a device that produces

a recognizable representation of a scene. An enhanced camera uses computation to improve some aspect of the camera, for example, reduce its physical depth while maintaining optical performance [17], [18], increase its spatial resolution [19], or expand its dynamic range [20]. Others have considered computation as a hybrid element to reduce or overcome aberrations [21], [22].

Computation has also been used to filter or accentuate information within a scene. For example, combining unique optics with post-detection processing allows one to extend an imager's depth of field [23]. Other examples include modulating a shutter during an exposure to reduce motion blur [24]. Computation in combination with new sensing modalities allows humans to "see" polarimetric information [25], spectral information [26], and three-dimensional information [27] in a manner similar to how they "see" through a human body using magnetic resonance.

With regard to enhancing cognition, some within the imaging community [28], [29] seek to extract information from scenes directly using physical means and post-detection processing but in a manner different from pure imaging processing, i.e., image detection followed by image processing, and from pure optical matched filtering. Such task-specific imagers require automatic feedback, dynamic elements, and adaptive processing to realize [29].

III. Computational mmW Imaging Approaches

Many mmW imaging systems have practical considerations that limit or preclude their use from surveillance and defense-related applications. In this section, we highlight several examples of computational mmW imaging methods that have been used to enhance imaging capabilities and to address some of these considerations, like size-weight-and-power (SWaP), imaging speed, and limited depth of field (DoF). These are important considerations for many potential applications, like stand-off imaging and surveillance of moving targets where high angular resolution, high image frame rates, and an extended DoF are keys to mission success. Computational imagers, like the distributed aperture imaging system discussed below, have also demonstrated promise in overcoming important SWaP-related issues. This is particularly important at millimeter wavelengths where high image resolution is typically achieved with large apertures and lens-based systems that scale volumetrically and can present challenges from a portability perspective.

A. Extended Depth-of-Field Imaging

Most mmW imaging systems have a narrow DoF, the distance over which an object is considered in focus. Consider the application of concealed weapon detection by imaging through clothing using mmW

imagers. If individuals are moving toward an imager through a corridor, the weapons will be visible only for the brief moment when they were in the DoF. This is one reason individuals are scanned in portals. However, extensions to scanning over a volume could provide scanning without creating bottlenecks, for example, in a public marketplace where security is important but a visible display of security might be counterproductive. Computational imaging methods [23], [30], [31] can be used to extend the DoF of mmW imaging systems. One such method was developed in [5] to extend the DoF of a passive mmW imaging system to allow for operation over a volume. In what follows, we review this computational imaging method for extending the DoF of a passive mmW imager.

In [5], a 94-GHz Stokes-vector radiometer was used to form images by raster scanning the system's single beam. One can model the 94-GHz imaging system as a linear, spatially incoherent, quasi-monochromatic system. The intensity of the detected image can be represented as a convolution between the intensity of the image predicted by the geometrical optics with the system point spread function [32]. Under these conditions, Eq. (1) is a valid representation with $\mathbf{H}$ the incoherent point spread function (PSF). $\mathbf{H}$ accounts for wave propagation through the aperture and is related to the magnitude square of the inverse Fourier transform of the system pupil function $P(u, v)$.

Displacement of an object from the nominal object plane of the imaging system introduces a phase error in the pupil function that increases the width of a point response and produces an out of focus image. For a 94 GHz imager with an aperture diameter $D = 24$" and object distance $d_o = 180$", $DoF \approx 17.4$" which ranges from 175.2" to 192.6". See Figure 4.

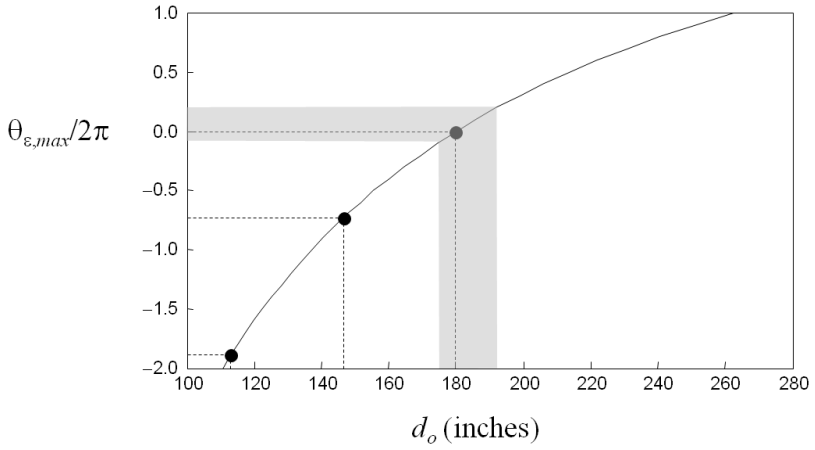

Fig. 4: Maximum relative pupil phase error as a function of object distance. The shaded region indicates a conventional depth of field.

The DoF of this imager was extended using a cubic phase element in conjunction with post-detection processing. The cubic phase element $P(u,v)$ is

$$P(u,v) = \exp[j\theta(u,v)]\mathrm{rect}\left(\frac{u}{W_u}, \frac{v}{W_v}\right), \tag{4}$$

where

$$\theta(u,v) = (\pi\gamma)\left[\left(\frac{2u}{W_u}\right)^3 + \left(\frac{2v}{W_v}\right)^3\right]$$

and rect is the rectangular function. The phase function is separable in the u and v spatial frequencies and has spatial extent W_u and W_v along the respective axis. The constant γ represents the strength of the cubic phase. Figure 5 shows the cubic phase element mounted on the antenna.

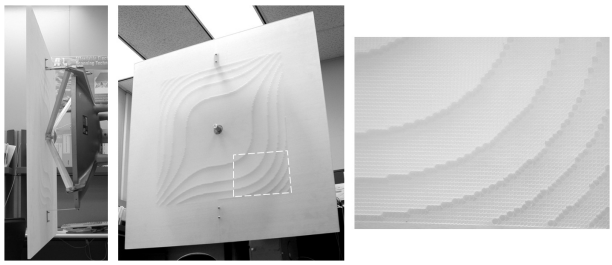

(a) (b) (c)

Fig. 5: Cubic phase element. (a) Side view of the cubic phase element mounted on the antenna. (b) Front view. (c) Detail of fabricated cubic phase element.

Figure 6 shows the measured PSFs for conventional imaging and imaging with a cubic phase. The width of the in-focus PSF at 180" is approximately 2 mm, which is consistent with a 1 mm pixel width. Note that the response of the cubic phase system is relatively unchanged, whereas the response of the conventional system changes considerably. A post-detection signal processing step is necessary to produce a well-defined sharp response [23], [30], [31].

If we assume Eq. (3) represents a linear post-detection process, we can implement $\mathbf{T}$ as a Wiener filter in Fourier space,

$$T(u,v) = \frac{H^*(u,v)}{|H(u,v)|^2 + \frac{K^{-2}\hat{\Phi}_N(u,v)}{\hat{\Phi_L}(u,v)}}, \tag{5}$$

where $H(u,v)$ is the optical transfer function associated with the cubic phase element, the parameter K is a measure of the signal-to-noise ratio, and the functions $\hat{\Phi}_L$ and $\hat{\Phi}_N$ are the expected power spectra of the object and noise, respectively. The optical transfer function is usually estimated from the experimentally measured point responses. One can view the estimated $i_p(x,y)$ as a diffraction limited response.

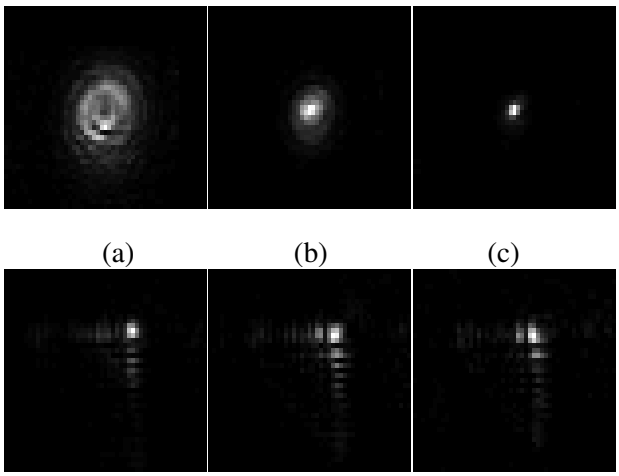

(a) (b) (c)

(d) (e) (f)

Fig. 6: Measured point spread functions for conventional imaging and imaging with a cubic phase. PSFs for conventional system at (a) 113”, (b) 146.5”, and (c) 180”. (d)-(f) PSFs for a system with cubic phase at the same distances for (a)-(c).

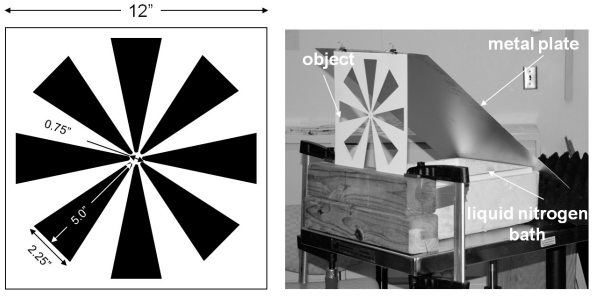

(a) (b)

Fig. 7: (a) Representation of the extended object used to compare conventional and cubic-phase imaging. (b) Schematic of object illumination [5].

The extended object used in the experiments is represented in Fig. 7(a). Images of an extended object for conventional imaging system at 113”,146” and 180” are shown in Fig. 8 (a)-(c), respectively. Each image is represented by 41×51 measurements, or pixels. The object size within the image is a function of optical magnification. Note that the conventional imaging system produces images with significant blurring. In contrast, even without signal processing, the images produced with cubic phase element retain more discernible characteristics of the object than the images from the conventional system, as

shown in Fig. 8 (d)-(f). It can be seen from Fig. 8 (g)-(i) that post processing compensates for the effect of the cubic phase element and retains frequency content that is otherwise lost in a conventional system. The wider bandwidth, in addition to the noise suppressing characteristics of the Weiner filter, produce images that appear sharper than those produced by a conventional imaging system. Hence, one can extend the region over which the system generates diffraction limited images. In fact, in, [5] it was shown that the DoF of a conventional 94-GHz imaging system can be extended from 17.4" to more than 68".

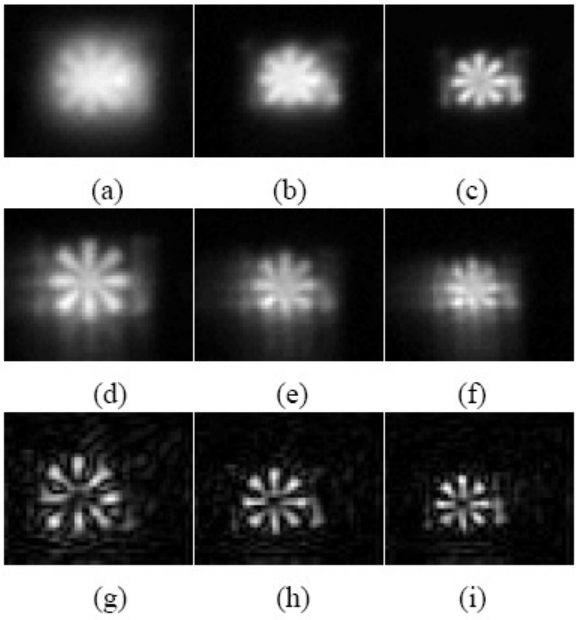

Fig. 8: Images from a conventional imaging system at (a) 113", (b) 146" and (c) 180". (d)-(f) Images from a system with cubic phase at the same object distances as for (a)-(c). (g)-(f) Processed images from a system with cubic phase at the same object distances as for (a)-(c) [9].

B. Distributed-Aperture mmW Imaging

Recently, a pupil plane, distributed aperture mmW imager was developed by the University of Delaware and Phase Sensitive Innovations [4] shown in Figure 9. As opposed to a continuous aperture over which radiation is collected to form an image, distributed aperture systems sample the incident radiation within subapertures. This is typically done when a continuous aperture is prohibitive due to scale, e.g., for radio telescopy. This approach was particularly taken for mmWs due to the lack of detection technology, such as inexpensive silicon-based detector arrays used for detecting visible radiation. This approach offers

important SWAP-related benefits compared with more traditional architectures like compound antenna systems and lens-based imagers, since the overall upconversion system size scales in 2D versus 3D.

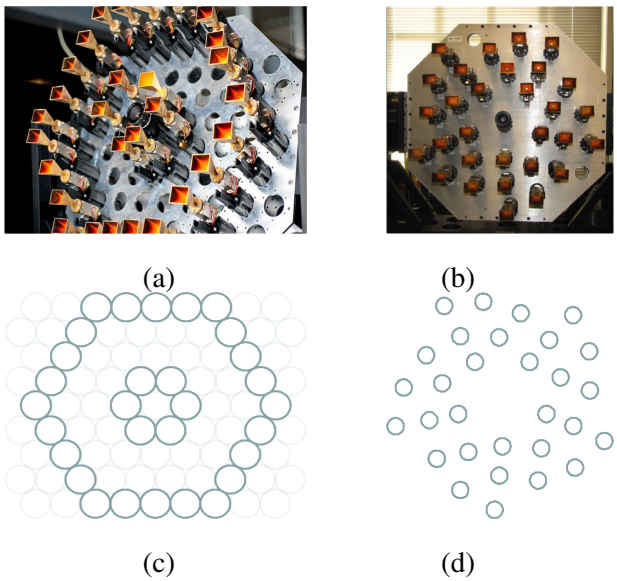

Fig. 9: 35-GHz 30-channel distributed aperture imaging system with (a) hexagonal and (b) nonredundant distributed apertures. Distributed aperture geometries for Hexagonal and Nonredundant apertures are shown in (c) and (d), respectively.

Image formation in a distributed array requires recording both magnitude and phase of the incident field at each subaperture and cross-correlating all the recorded, complex information. Typically, systems distribute a local oscillator to down-convert the captured field data to a lower intermediate frequency where it can be digitally recorded and processed. Although well suited for imaging at microwave frequencies, at mmW frequencies the power, size, and space requirements for distributing the local oscillator, the intermediate frequency processing, and construction of the correlation engines present significant design challenges, which increase cost.

It was shown in [4] that these challenges can be overcome by up-converting to optical frequencies and taking advantage of existing optical technology for processing and imaging. Electro-optic modulators were used to modulate received millimeter-wave radiation onto the sidebands on an optical carrier [33]. Optical up-conversion allows one to use lightweight, flexible fiber optics to route optical energy before and after mmW encoding, which eliminates the need for cables to distribute a local oscillator.

Even more significant, optical up-conversion allows one to use an optical lens to perform the necessary correlation required for image formation. Digital reconstruction requires discrete spatial Fourier transforms

and correlations, the number of which increases quadratically with the number of subapertures. The phase transformation of a lens combined with propagation over a distance generates physically the correlations necessary for image formation.

Thus, in brief, the system proposed in [4], samples discretely the complex wave-amplitude of a mmW signal and converts the mmW signal to an optical one using electro-optical modulators while preserving the spatial distribution of samples using an optical fiber array. The output of the fiber array is spatially Fourier transformed using a lens and the resulting optical image is captured using an optical detector array or CCD. One of the important features of this imager is that the imager volume does not scale with the aperture diameter as the scale of the image-forming elements is fixed.

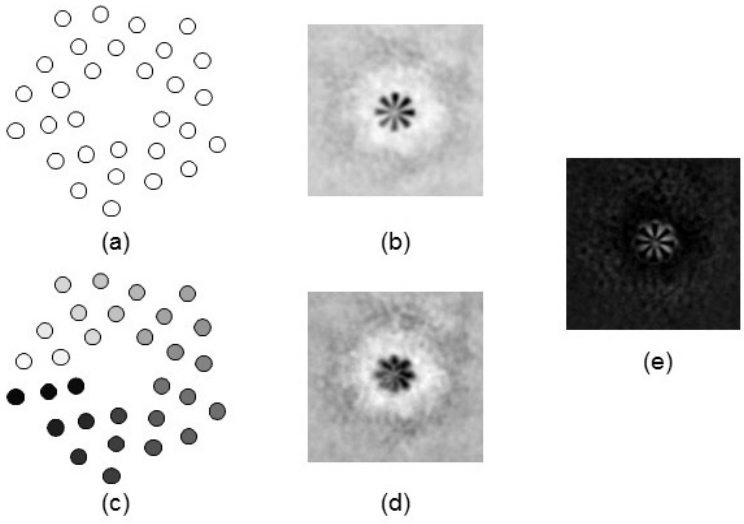

Fig. 10: Edge detection performed using a nonredundant distributed aperture. (a) Aperture phase and (b) corresponding image of an extended object assuming zero aperture phase. (c) and (d) Same as in (a) and (b) except with circular phase across the aperture. White represents 0-phase and black, 2π-phase. Intermediate grey colors represent phases between 0 and 2π. (e) Difference between (b) and (d) [7].

Another significant feature of this imager is its ability to control the relative phase of each receiving element in the distributed aperture, which provides electronic control of the imager's PSF. It allows multi-domain sensing by simultaneous and independent manipulation of both the Fourier and image planes of the system. This is a unique capability that permits one to change the imager's PSF on-the-fly and enables rapid sparse sampling of desired target by electronically steering the beam in a manner similar to a phased array antenna. Analysis of the imager as an incoherent imaging system highlights the link

between element phase and PSF [7]. It was shown in [7] that by modifying the aperture phases of the hexagonal and nonredundant distributed aperture systems, one can perform low-resolution analog image processing. The simplest approach could be to take the difference between two images of the same object captured using two different pupil functions,

$$f(x,y) = f_+(x,y) - f_-(x,y), \tag{6}$$

where $o(x,y)$ is the input object and

$$f_+(x,y) = o(x,y) * *h_+(x,y) \tag{7}$$

$$f_-(x,y) = o(x,y) * *h_-(x,y). \tag{8}$$

For example, one can construct a one-dimensional bandpass filter by manipulating the phase functions. To understand this heuristically, one can model the corresponding PSFs as δ-functions

$$h_+(x,y) = \delta(x,y), \tag{9}$$

$$h_-(x,y) = \frac{1}{2}[\delta(x-x_0,y) + \delta(x+x_0,y)], \tag{10}$$

to approximate the composite transfer function $H(u,v)$ as

$$H(u,v) = H_+(u,v) - H_-(u,v) = 1 - \cos(2\pi x_0 u), \tag{11}$$

which filters low spatial frequencies and passes frequencies centered at $u = 1/x_0$. Such filtering can be useful for edge detection. See Fig. 10. Furthermore, it was shown in [34] that phase can also be used to do more complex signal processing such as reducing noise. Figure 11 illustrates the real-time nature of the imager where a person behind a plywood is imaged at a video-rate.

C. Compressive mmW Imagers

Compressive sensing (CS) is an important tool that has shown promise in overcoming some of the common limitations associated with mmW imaging. For example, a wide field of regard and high image frame rates are desired for many applications, like stand-off imaging of moving targets. Because large-format arrays present cost challenges due to technological hurdles like availability of cost-effective and powerful source technology and sensitive, low-cost detectors, many current systems use a single element or a small array in combination with a compound antenna system to scan a larger scene and build up an image (e.g., [35], [36], [37], [38]). These architectures can present challenges to achieving the video frame rates required for some imaging applications [38]. As highlighted in this section, mmW CS techniques

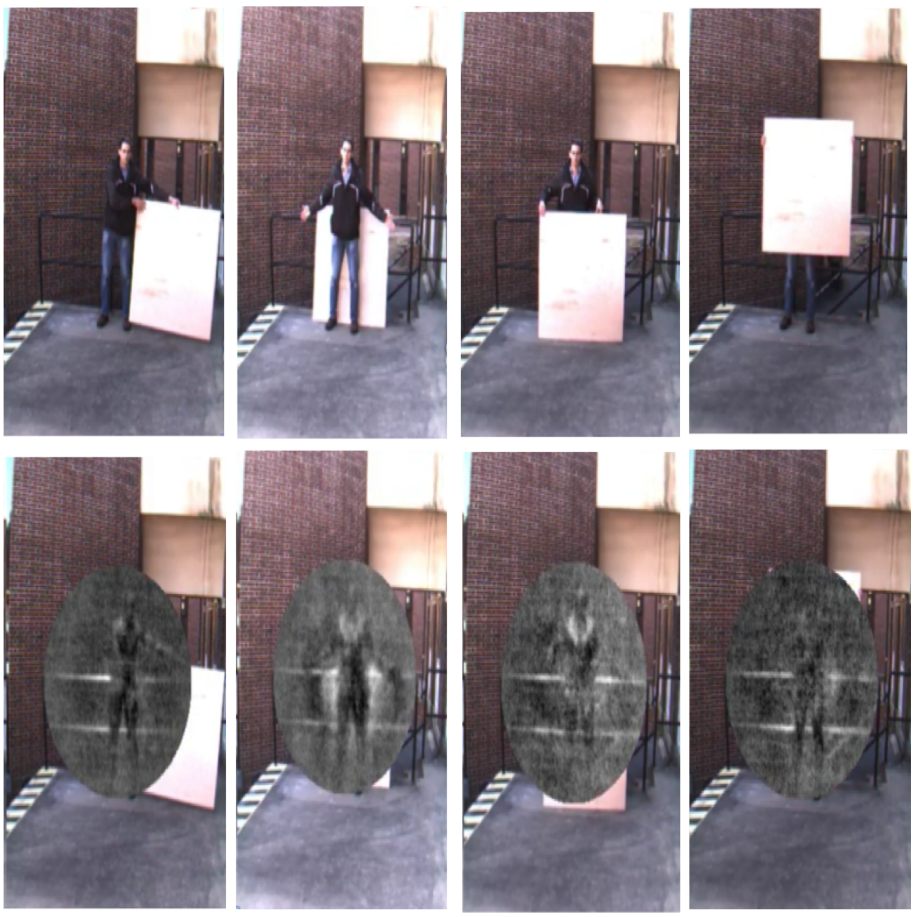

Fig. 11: Real-time, video snap-shots seeing through 1/4 inch plywood.

have shown promise in overcoming issues like high frame-rate challenges by potentially reducing the overall number of scene measurements needed to reconstruct an image.

Compressive sensing can be viewed as a special case of computational imaging in which partial or low-dimensional measurements are obtained by designing a specific sensing modality. In this case, the measurement matrix $\mathbf{H}$ in (1) has more columns than rows and a nonlinear recovery algorithm is used to reconstruct the scene [39], [40]. A number of CS methods have been developed to reduce the acquisition time of mmW imagers [8]–[11], [41]. For instance, [10] proposed a compressive passive mmW imaging method in which randomly encoded masks are employed at the focal plane of the imager to acquire incoherent measurements of the imaged scene. A Bayesian reconstruction algorithm was developed to estimate the original image from these compressive measurements. It was shown that this system can significantly reduce the number of required measurements for passive mmW imaging. This method was

later extended in [42] by constructing a single unified and compact mask such that no mechanical mask exchange is necessary for collecting compressive measurements.

Another method based on CS for terahertz (THz) imaging was proposed in [11]. This method uses a single pixel detector in combination with a series of random masks to enable high-speed image acquisition. It was shown that this system is capable of producing 32×32 images of complex objects with only 300 (approximately 30%) measurements. Rather than using random masks, [43] proposes to use Toeplitz matrix-based masks. This method has the advantage that a large number of masks can be represented by a single sensing mask. It was shown that the image acquisition time of this system is only limited to the speed of the THz detector.

A mmW imaging modality with extended DoF with reduced spatial sampling was developed in [8], [9]. This method essentially uses a cubic phase element at the pupil of the imager while collecting partial measurements. The image is then recovered by using a non-linear reconstruction algorithm. It was shown that one can achieve a greater than four-fold increase in DoF with a reduction in sampling requirements by a factor of at least two by using this system.

In a recent work [44], active matamaterials were introduced as real-time tunable, spectrally sensitive spatial masks for single pixel THz imaging. This method requires no moving parts and can yield improved signal-to-noise ratios over standard raster-scanning techniques for THz imaging. Furthermore, it was demonstrated that the use of this technique in the CS framework can allow one to acquire high-frame-rate and high-fidelity images.

IV. Discussion and Concluding Remarks

This article presented a review of recent developments in mmW imaging based on computational imaging methods for security and surveillance applications. We believe that recent advances in computational imaging have brought substantial opportunities to mmW imaging. We hope that the survey has helped to guide the interested reader through the extensive literature. It does not cover all the literature on mmW and computational imaging, so we have chosen to focus on a subset of work that reflects some of the most recent progress.

A number of challenges and issues commonly confront mmW imaging technology. Computational imaging methods may prove useful in addressing some of these challenges. Below, we list several examples

- *Affordability.* The technology readiness level of mmW devices is immature compared with optical and infrared arrays. The lack of readily available and affordable sources and detection technology

has resulted in comparatively small arrays (kilopixels or fewer) and a trade-off between number of achievable image pixels and the desire to rapidly image wide fields of regard with high angular resolution. Millimeter wave compressed sensing has shown promising results in reducing the overall number of scene observations needed to reconstruct an image. Perhaps these techniques or other computational imaging methods could help curb the cost of mmW systems by requiring fewer detector elements to realize an imaging capability that is more comparable to what could be achieved with a larger-format array.

- *SWaP.* Many mmW imaging systems are not viable for deployment across a broad variety of platforms that would benefit from their use. Compound antenna systems and lens-based imagers, for example, scale volumetrically. To achieve high resolution and wide field of view, one typically uses larger apertures and mechanical scanners, which have important implications for SWaP. These solutions do not tend to be man-portable, for example. Additionally, for broad applicability, one also wants platform-agnostic solutions that do not require specific aspects of the platform to form images, like platform motion, for example. Computational imagers may offer some key advantages, like the distributed aperture mmW imaging technology discussed in Section III which scales in 2D versus 3D, for example.
- *Surveillance of moving targets.* Imaging of moving targets with high resolution and high frame rates can be challenging with existing systems. At lower frequency, SAR offers excellent atmospheric penetration properties but relatively slow frame rates. Millimeter wave imagers can be limited by the speed of mechanical scanners, and electronic beam-scanning technology is immature and costly at millimeter wavelengths. Given challenges like these, perhaps computational imaging techniques could be applied to help compensate for image blur with existing systems.

Computational mmW imaging promises to be an active area of research. However, little is known about the quantitative performance advantage of computational imaging methods for mmW imaging. We expect that derivation of the performance bounds for various computational mmW imaging methods will produce stronger guidance to developing more advanced mmW imaging modalities which will have a wider spectrum of applications in surveillance, defense and aviation problems.

AUTHOR BIOGRAPHIES

Vishal M. Patel (Ph.D., UMD, 2010) received the B.S. degrees in electrical engineering and applied mathematics (Hons.) and the M.S. degree in applied mathematics from North Carolina State University, Raleigh, NC, USA, in 2004 and 2005, respectively, and the Ph.D. degree in electrical engineering from

the University of Maryland College Park, MD, USA, in 2010. He is currently an Assistant Professor in the Department of Electrical and Computer Engineering (ECE) at Rutgers University. Prior to joining Rutgers University, he was a member of the research faculty with the University of Marylands Institute for Advanced Computer Studies, College Park, MD, USA. His current research interests include signal processing, computer vision, and pattern recognition with applications in biometrics and imaging. He is a recipient of the 2016 ONR Young Investigator Award and the 2010 ORAU Post-Doctoral Fellowship. He is a member of Eta Kappa Nu, Pi Mu Epsilon, and Phi Beta Kappa.

Joseph N. Mait (Ph.D., GA Tech, 1985) is Chief Scientist of the US Army Research Laboratory. He is a Fellow of SPIE and OSA, and a senior member of IEEE. He is the immediate past Editor-in-Chief of OSA's Applied Optics. In 2014 he was awarded a Presidential Rank Award for Meritorious Senior Professionals. Dr. Mait's research interests include sensors and the application of optics, photonics, and electro-magnetics to sensing and sensor signal processing.

Dennis W. Prather (Ph.D., UMD, 1997) is an Endowed Professor of Electrical Engineering at the University of Delaware. He is a senior member of the IEEE, Fellow of the Society of Photo-Instrumentation Engineers (SPIE) and a Fellow of the Optical Society of America (OSA). His research focuses on both the theoretical and experimental aspects of RF-photonic elements and their integration into various systems for imaging, communications and Radar. He has authored or co-authored over 400 scientific papers, holds over 40 patents, and has written 10 books/book-chapters.

Abigail S. Hedden (Ph.D., University of Arizona, 2007) is a physicist in the RF Technology and Integration Branch of the Sensors and Electron Devices Directorate at the U.S. Army Research Laboratory in Adelphi, MD. Current research interests include development of millimeter-wave instrumentation and radar systems, phenomenology, and experimentation.

REFERENCES

[1] R. Appleby and R. N. Anderton, "Millimeter-wave and submillimeter-wave imaging for security and surveillance," *Proceedings of the IEEE*, vol. 95, no. 8, pp. 1683–1690, Aug 2007.

[2] L. Yujiri, M. Shoucri, and P. Moffa, "Passive millimeter wave imaging," *IEEE Microwave Magazine*, vol. 4, no. 3, pp. 39–50, Sept 2003.

[3] J. P. Wilson, D. G. Mackrides, J. P. Samluk, and D. W. Prather, "Comparison of diurnal contrast changes for millimeter-wave and infrared imagery," *Applied Optics*, vol. 49, no. 19, pp. E31–E37, Jul 2010.

[4] R. Martin, C. A. Schuetz, T. E. Dillon, C. Chen, J. Samluk, E. L. Stein, M. Mirotznik, and D. W. Prather, "Design and performance of a distributed aperture millimeter-wave imaging system using optical upconversion," in *Proceedings of SPIE*, 2009, pp. 7309–08.

[5] J. N. Mait, D. A. Wikner, M. S. Mirotznik, J. van der Gracht, G. P. Behrmann, B. L. Good, and S. A. Mathews, "94-ghz imager with extended depth of field," *IEEE Transactions on Antennas and Propagation*, vol. 57, no. 6, pp. 1713–1719, June 2009.

[6] A. S. Hedden, C. R. Dietlein, and D. A. Wikner, "Design of 220-ghz electronically scanned reflectarrays for confocal imaging systems," *Optical Engineering*, vol. 51, no. 9, pp. 091 611–1–091 611–10, Sept 2012.

[7] J. N. Mait, R. D. Martin, C. A. Schuetz, and D. W. Prather, "Millimeter wave imaging with engineered point spread functions," *Optical Engineering*, vol. 51, no. 9, pp. 091 606–1–091 606–9, Sept 2012.

[8] V. M. Patel and J. N. Mait, "Passive millimeter-wave imaging with extended depth of field and sparse data," in *IEEE International Conference on Acoustics, Speech and Signal Processing*, March 2012, pp. 2521–2524.

[9] ——, "Compressive passive millimeter-wave imaging with extended depth of field," *Optical Engineering*, vol. 51, no. 9, pp. 091 610–1–091 610–7, Sept 2012.

[10] S. D. Babacan, M. Luessi, L. Spinoulas, A. K. Katsaggelos, N. Gopalsami, T. Elmer, R. Ahern, S. Liao, and A. Raptis, "Compressive passive millimeter-wave imaging," in *IEEE International Conference on Image Processing*, Sept 2011, pp. 2705–2708.

[11] W. L. Chan, K. Charan, D. Takhar, K. F. Kelly, R. G. Baraniuk, and D. M. Mittleman, "A single-pixel terahertz imaging system based on compressed sensing," *Applied Physics Letters*, vol. 93, no. 12, 2008.

[12] J. P. Wilson, C. A. Schuetz, T. E. Dillon, P. Yao, C. E. Harrity, and D. W. Prather, "Passive 77 ghz millimeter-wave sensor based on optical upconversion," *Applied Optics*, vol. 51, no. 18, pp. 4157–4167, Jun 2012.

[13] J. Hunt, J. Gollub, T. Driscoll, G. Lipworth, A. Mrozack, M. S. Reynolds, D. J. Brady, and D. R. Smith, "Metamaterial microwave holographic imaging system," *Journal of the Optical Society of America A*, vol. 31, no. 10, pp. 2109–2119, Oct 2014.

[14] M. Bertero and P. Boccacci, *Introduction to inverse problems in imaging*. Bristol, UK Philadelphia, Pa. Institute of Physics Pub. cop., 1998.

[15] O. Cossairt, M. Gupta, and S. K. Nayar, "When does computational imaging improve performance?" *IEEE Transactions on Image Processing*, vol. 22, no. 2, pp. 447–458, Feb 2013.

[16] A. V. Lugt, "Signal detection by complex spatial filtering," *IEEE Transactions on Information Theory*, vol. 10, no. 2, pp. 139–145, Apr 1964.

[17] J. Tanida, T. Kumagai, K. Yamada, S. Miyatake, K. Ishida, T. Morimoto, N. Kondou, D. Miyazaki, and Y. Ichioka, "Thin observation module by bound optics (tombo): Concept and experimental verification," *Appl. Opt.*, vol. 40, pp. 1806–1813, 2001.

[18] M. Shankar, R. Willett, N. Pitsianis, T. Schulz, R. Gibbons, R. T. Kolste, J. Carriere, C. Chen, D. Prather, and D. Brady, "Thin infrared imaging systems through multichannel sampling," *Appl. Opt.*, vol. 47, pp. B1–B10, 2008.

[19] S. S. Young and R. G. Driggers, "Superresolution image reconstruction from a sequence of aliased imagery," *Appl. Opt.*, vol. 45, pp. 5073–5085, 2006.

[20] M. Mirotznik, S. Mathews, R. Plemmons, P. Pauca, T. Torgersen, R. Barnard, B. Gray, T. Guy, Q. Zhang, J. van der Gracht, C. Petersen, M. Bodnar, and S. Prasad, "A practical enhanced-resolution integrated optical-digital imaging camera (periodic)," in *Modeling and Simulation for Military Operations IV, D. A. Trevisani, ed., Proc. SPIE 7348*, 2009, p. 734806.

[21] E. R. Dowski and K. S. Kubala, "Reducing size, weight, and cost in a lwir imaging system with wavefront coding," in *Infrared Imaging Systems: Design, Analysis, Modeling, and Testing XV, G. C. Holst, ed., Proc. SPIE 5407*, 2004, pp. 66–73.

[22] D. G. Stork and M. D. Robinson, "Theoretical foundations for joint digital-optical analysis of electro-optical imaging systems," *Appl. Opt.*, vol. 47, pp. B64–B75, 2008.

[23] E. R. Dowski and W. T. Cathey, "Extended depth of field through wave-front coding," *Appl. Opt.*, vol. 34, no. 11, pp. 1859–1866, Apr. 1995.

[24] A. Agrawal, Y. Xu, and R. Raskar, "Invertible motion blur in video," in *ACM Transactions on Graphics - Proceedings of ACM SIGGRAPH 2009*, 2009, p. 28.

[25] J. S. Tyo, D. L. Goldstein, D. B. Chenault, and J. A. Shaw, "Review of passive imaging polarimetry for remote sensing applications," *Appl. Opt.*, vol. 45, pp. 5453–5469, 2006.

[26] M. Gehm, R. John, D. J. Brady, R. Willett, and T. Schulz, "Single-shot compressive spectral imaging with a dual-disperser architecture," *Opt. Express*, vol. 15, pp. 14 013–14 027, 2007.

[27] T.-C. Poon, B. Lee, H. Yoshikawa, and J. Rosen, "Digital holography and 3-d imaging: feature introduction," *Appl. Opt.*, vol. 48, p. DH2, 2009.

[28] M. A. Neifeld and P. Shankar, "Feature-specific imaging," *Appl. Opt.*, vol. 42, pp. 3379–3389, 2003.

[29] M. P. Christensen, V. Bhakta, D. Rajan, T. Mirani, S. C. Douglas, S. L. Wood, and M. W. Haney, "Adaptive flat multiresolution multiplexed computational imaging architecture utilizing micromirror arrays to steer subimager fields of view," *Appl. Opt.*, vol. 45, pp. 2884–2892, 2006.

[30] W. T. Cathey and E. R. Dowski, "New paradigm for imaging systems," *Appl. Opt.*, vol. 41, no. 29, pp. 6080–6092, Oct. 2002.

[31] S. Bradburn, W. T. Cathey, and E. R. Dowski, "Realizations of focus invariance in optical–digital systems with wave-front coding," *Appl. Opt.*, vol. 36, no. 35, pp. 9157–9166, Dec. 1997.

[32] J. W. Goodman, *Introduction to Fourier optics*. Englewood, CO, USA: Roberts and Company, 2005.

[33] C. A. Schuetz and D. W. Prather, "Optical upconversion techniques for high-sensitivity millimetre-wave detection," in *Proceedings of SPIE: Passive Millimetre-Wave and Terahertz Imaging and Technology*, 2004, pp. 166–174.

[34] J. N. Mait, R. D. Martin, C. A. Schuetz, S. Shi, D. W. Prather, P. F. Curt, and J. Bonnett, "Minimum bias design for a distributed aperture millimeter wave imager," in *IEEE Global Conference on Signal and Information Processing*, 2013.

[35] K. B. Cooper, "Imaging, doppler, and spectroscopic radars from 95 to 700 ghz," pp. 983 005–983 005–9, 2016.

[36] E. Gandini and N. Llombart, "Toward a real time stand-off submillimeter-wave imaging system with large field of view: quasi-optical system design considerations," pp. 946 205–946 205–12, 2015.

[37] K. B. Cooper, R. J. Dengler, N. Llombart, B. Thomas, G. Chattopadhyay, and P. H. Siegel, "Thz imaging radar for standoff personnel screening," *IEEE Transactions on Terahertz Science and Technology*, vol. 1, no. 1, pp. 169–182, Sept 2011.

[38] N. Llombart, R. J. Dengler, and K. B. Cooper, "Terahertz antenna system for a near-video-rate radar imager [antenna applications]," *IEEE Antennas and Propagation Magazine*, vol. 52, no. 5, pp. 251–259, Oct 2010.

[39] Y. Eldar and G. Kutyniok, *Compressed Sensing: Theory and Applications*, ser. Compressed Sensing: Theory and Applications. Cambridge University Press, 2012. [Online]. Available: https://books.google.com/books?id=Gm3ihcJwN0YC

[40] V. M. Patel and R. Chellappa, *Sparse representations and compressive sensing for imaging and vision*. SpringerBriefs, 2013.

[41] C. Fernandez-Cull, D. A. Wikner, J. N. Mait, M. Mattheiss, and D. J. Brady, "Millimeter-wave compressive holography," *Applied Optics*, vol. 49, no. 19, pp. E67–E82, Jul 2010.

[42] L. Spinoulas, J. Qi, A. K. Katsaggelos, T. W. Elmer, N. Gopalsami, and A. C. Raptis, "Optimized compressive sampling for passive millimeter-wave imaging," *Applied Optics*, vol. 51, no. 26, pp. 6335–6342, Sep 2012.

[43] A. Heidari and D. Saeedkia, "A 2d camera design with a single-pixel detector," in *International Conference on Infrared, Millimeter, and Terahertz Waves*, 2009, pp. 1–2.

[44] C. M. Watts, D. Shrekenhamer, J. Montoya, G. Lipworth, J. Hunt, T. Sleasman, S. Krishna, D. R. Smith, and W. J. Padilla, "Terahertz compressive imaging with metamaterial spatial light modulators," *Nature Photonics*, vol. 8, pp. 605–609, June 2014.